21st Australasian Fluid Mechanics Conference
Adelaide, Australia
10-13 December 2018

Sensitivity of HF Radar Signatures of Ship Wakes to Hull Geometry Parameters

S.J. Anderson

Department of Physics
University of Adelaide, South Australia 5005, Australia

Abstract

There is a lot of interest in wake detection from a surveillance perspective, especially for the case of submarines, but there is also strong motivation to study ship wakes from the perspective of ocean hydrodynamics. It is now well established that nonlinear processes play a central role in the geometry and the temporal evolution of ocean wave fields, but the investigation of these mechanisms in the open sea must contend with the simultaneous presence of many wave components and hence a large number of unknowns in any parametrisation of the dynamical behaviour of the surface. If it were possible to introduce a known, deterministic element to the system of waves, one might be able to isolate particular interactions and solve for the parameters of interest. In this paper we take a first step towards this objective by exploring the sensitivity of HF radar signatures to hull geometry.

Introduction

The wake produced by a moving ship consists of several components, but of these only one can register a distinctive signature to an HF radar, namely, the Kelvin wake. Fortuitously, the spatio-temporal properties of the Kelvin wake are well matched to those of the ambient waves whose nonlinear dynamics are of interest. Building on recent studies of the HF radar signatures of ship wakes [1], we propose here the use of ship Kelvin wakes as a controllable input to the wave system, whose response can then be observed with HF radar, yielding information about the nonlinear dynamics. This approach to system identification is most familiar in the case of linear systems and the mapping of Green's functions but is also widely practised for nonlinear systems, especially via Volterra series models.

The prospects for success of the proposed methodology rest heavily on the accuracy with which we can model the wake and hence the sensitivity of the wake pattern to the geometry of the hull, but, just as importantly, they depend on the way *that* sensitivity maps onto the space of radar signatures. Those signatures are a function of both the wake and the ambient sea; the precision of radar measurement and the fidelity of the inversion procedure are the ultimate determinants of our ability to isolate and measure the interaction mechanisms.

As one further step towards the development of the proposed technique, we have carried out modelling of the sensitivity of the HF radar signatures to variations in hull geometry, side-stepping the intermediate issue of the fidelity of the wake model. We argue that the observed verisimilitude of parametric wake models when compared with imagery justifies this approach : while detailed CFM modelling may yield slightly different wake predictions, the differential effects should be of comparable magnitude.

In this paper we present (i) some examples of computed radar signatures of wakes for different hull parameters, demonstrating the prospects for ship discrimination, and (ii) isolate the contributions due to nonlinear wake-sea interactions which may provide a window into nonlinear wave-wave interactions in the open sea.

Wakes and their structure

A localised pressure distribution in uniform translational motion across or within the sea results in a variety of disturbances in the fluid. At HF, the dominant contribution to the overall signature comes from the Kelvin wake, to which we will restrict attention here

As pointed out in [2], the Kelvin wake can be interpreted as a form of Cerenkov radiation but, unlike most forms of the latter, its angular distribution is greatly broadened by the strongly dispersive nature of deep water gravity waves. Moreover, the angular spectrum is naturally partitioned into transverse and diverging parts, associated with the two roots of a characteristic equation and possessing different exponents of asymptotic decay with distance. The Kelvin wake is of invariant form in the reference frame of the ship, and this constrains the spectral components to lie on a characteristic curve; other invariant features exist, indicated in Figure 1 which presents a schematic of a conventional wake with both component wave fields evident along with the Kelvin angle, 19°28′, and the angle of the diverging wave crest normal, 35°16′.

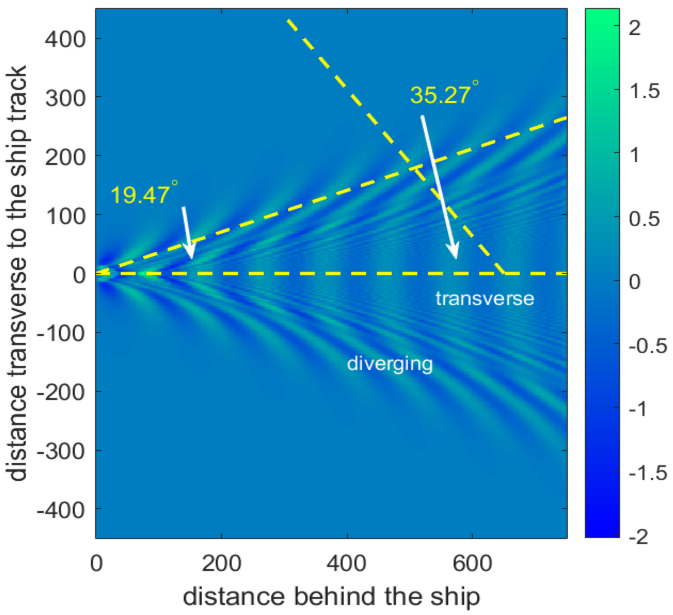

Figure 1. A schematic representation of the Kelvin wake showing the principal invariants

Modelling the Kelvin wake

Within the domain of linearized hydrodynamics in an inviscid fluid, the irrotational flow produced by any pressure distribution can be generated by a distribution of Havelock sources, which are point sources in the presence of the free planar surface,

$$G(x,y,z;\zeta) = -\frac{1}{4\pi r} + \frac{1}{4\pi^2}\Re\int_{-\pi/2}^{\pi/2}\int_0^\infty e^{-i\kappa(x\cos\theta+y\sin\theta)}\frac{\kappa+\kappa_0 sec^2\theta}{\kappa-\kappa_0 sec^2\theta}e^{\kappa(z+\zeta)}dkd\theta$$

where $\kappa_0 = \frac{g}{U^2}$.

To apply this representation, one is obliged to introduce approximations, which can be done in various ways. In the present study, so far, we have employed the Michell-Kelvin ("thin ship") approximation, which models the disturbance due to the body by a specified continuous distribution of singularities along the center-plane of the body, also assuming that the kinematic and dynamic free surface boundary conditions can be approximated by a linearised condition on the plane equilibrium surface [3]. The strength of the singularities is proportional to the axial derivative of the hull contour. For the latter, in the absence of really detailed hull profiles, we have fitted a parametric warship model to the overall dimensions. Nothing is sacrificed by use of such a model in the present context. Then we have

$$\eta(x,y) = -\frac{2}{\kappa_0}\iint_R Y_\xi(\xi,\zeta)G_x(x-\xi,y,z;\zeta)\,d\xi d\zeta$$

As discussed in [4], this four-dimensional integral is numerically challenging, but considerable reduction in computational load can be achieved by re-ordering the integration, arriving at

$$\eta(x,y) = \frac{1}{\pi^2}\Re\int_{-\pi/2}^{\pi/2}\int_0^\infty e^{-i\kappa(x\cos\theta+y\sin\theta)}\frac{\kappa^2(P+iQ)}{\kappa-\kappa_0 sec^2\theta}d\kappa d\theta$$

where

$$P+iQ = -\frac{1}{ik\cos\theta}\iint Y_\xi(\xi,\zeta)e^{i\kappa\cos\theta\,\xi+\kappa\zeta}d\xi d\zeta$$

In the far field, most contribution comes from the pole at $\kappa = \kappa_0 sec^2\theta$, so we can write

$$\eta(x,y) = -\frac{2\kappa_0^2}{\pi}\Re\, i\int_{-\pi/2}^{\pi/2}\int_0^\infty e^{-i\kappa(x\cos\theta+y\sin\theta)}sec^4\theta \times (P+iQ)d\kappa d\theta$$

Now, this can be written compactly as

$$\eta(x,y) = \Re\int_{-\pi/2}^{\pi/2}A(\theta)e^{-i\kappa(x\cos\theta+y\sin\theta)}d\theta$$

which we immediately recognise as a spectral representation. This is exactly what we want for our HF radar signature calculation because the scattering theory we use to compute the Doppler spectrum of HF sea clutter uses spectral representations as input. Specifically, we need only to compute the power spectrum,

$$S(\vec{\kappa}) = |A(\theta)|^2$$

then we are ready to calculate the radar signature. And as a bonus, the wave resistance to the ship's motion, and hence the power radiated into the wake, is given by the famous Michell formula,

$$R = \frac{\pi}{2}\rho U^2\int_{-\pi/2}^{\pi/2}|A(\theta)|^2\cos^3\theta d\theta$$

To be of significant value to us, the wake spectrum, and ultimately its signature, will need to vary appreciably with ship speed and hull geometry. To demonstrate that this is the case, Figure 2 shows the angular spectrum of a particular frigate at a range of speeds. The distribution of energy varies markedly, with transverse and diverging fields taking turns to dominate as speed increases.

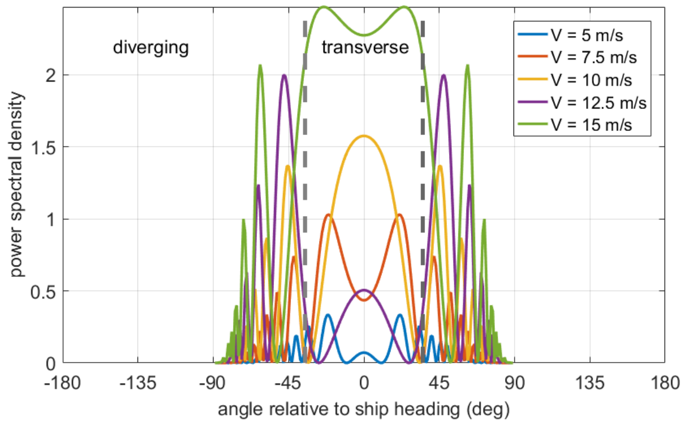

Figure 2. Angular spectra of a ship wake computed at five speeds to show the variation in azimuthal distribution

We have explored the dependence on hull geometry by examining a realistic scenario : the need to discriminate between two vessels that have similar dimensions. In Figure 3, we plot the elevation pattern of SHIP A at four speeds. Then, in Figure 4, we do the same for SHIP B. The differences are easily observed by the human eye, but we must establish that the same is true for an HF radar.

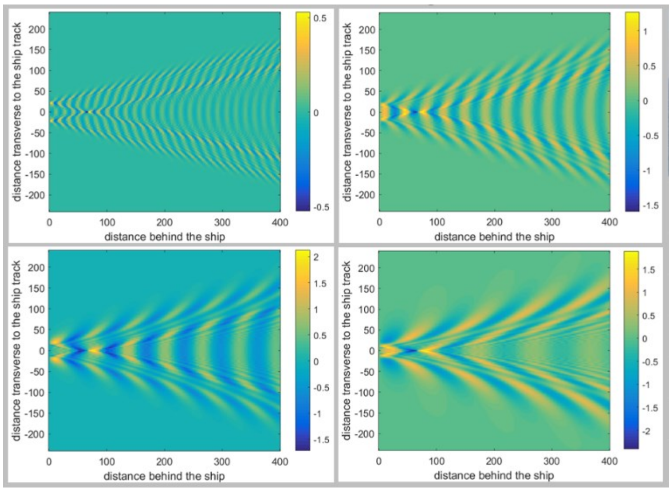

Figure 3. Computed wake elevation patterns of Frigate A at speeds of 10, 15, 20 and 25 knots

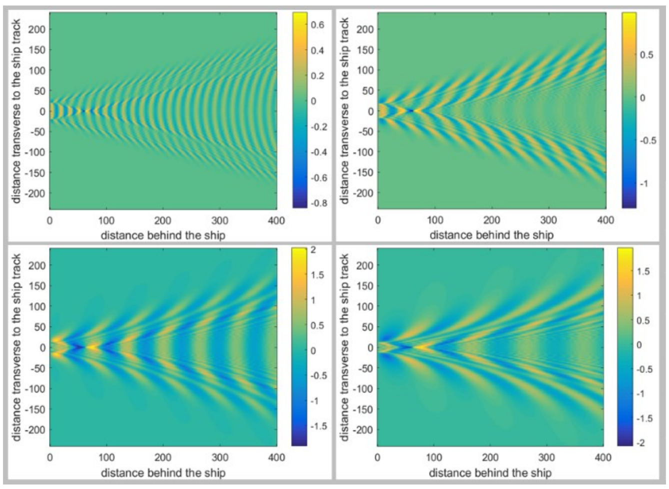

Figure 4. Computed wake elevation patterns of Frigate B at speeds of 10, 15, 20 and 25 knots

HF scattering from composite sea surfaces

The most widely used theoretical treatment of HF scattering from the time-varying sea surface is the small perturbation theoretic model developed by Barrick [5] based on the Rayleigh-Rice method. We employ a generalized theory that is based on the same assumptions but extends the standard theory to handle arbitrary bistatic angles, arbitrary elevation angles and arbitrary polarizations [6]. This is important as the ability to detect wakes is predicted to be enhanced if bistatic radar configurations are employed.

From the scattering theory, the Doppler spectrum imposed on an HF signal arriving at the cell of interest with wavevector $\vec{k}_{inc}$ and departing with wavevector $\vec{k}_{scat}$ can be written as

$$\tilde{D}(\vec{k}_{scat},\vec{k}_{inc};\omega) = \int d\vec{\kappa}_1 F_1(\vec{k}_{scat},\vec{k}_{inc},\vec{\kappa}_1)S(\vec{\kappa}_1) + \iint d\vec{\kappa}_1 d\vec{\kappa}_2 F_2(\vec{k}_{scat},\vec{k}_{inc},\vec{\kappa}_1,\vec{\kappa}_2)S(\vec{\kappa}_1)S(\vec{\kappa}_2)$$

where F_1 and F_2 are the kernels for first and second order scatter in the perturbation theoretic formulation and $S(\vec{\kappa})$ is the directional wave spectrum.
The kernels can be factorised into two types of term : (i) core functions Γ_1 and Γ_2 describing the first and second order electromagnetics and hydrodynamics in general form, and (ii) the delta functions that express the dispersion relation and the scattering geometry,

$$F_1(\vec{k}_{scat},\vec{k}_{inc},\vec{\kappa}_1) = \Gamma_1(\vec{k}_{scat},\vec{k}_{inc},\vec{\kappa}_1)\delta(\vec{k}_{scat}-\vec{k}_{inc}\pm\vec{\kappa}_1)\times \delta(\omega\pm\Omega(\vec{\kappa}_1))$$

$$F_2(\vec{k}_{scat},\vec{k}_{inc},\vec{\kappa}_1,\vec{\kappa}_2) = \Gamma_2(\vec{k}_{scat},\vec{k}_{inc},\vec{\kappa}_1,\vec{\kappa}_2)\times \delta(\vec{k}_{scat}-\vec{k}_{inc}\pm\vec{\kappa}_1\pm\vec{\kappa}_2)\times \delta(\omega\pm\Omega(\vec{\kappa}_1)\pm\Omega(\vec{\kappa}_2))$$

Recall that

$$S(\vec{\kappa}) = S_{wake}(\vec{\kappa}) + S_{wave}(\vec{\kappa})$$

and substitute in the expression for the Doppler spectrum :

$$\tilde{D}(\vec{k}_{scat},\vec{k}_{inc};\omega) = \int d\vec{\kappa}_1 F_1(\vec{k}_{scat},\vec{k}_{inc},\vec{\kappa}_1)[S_{wake}(\vec{\kappa}_1)+S_{wave}(\vec{\kappa}_1)] + \iint d\vec{\kappa}_1 d\vec{\kappa}_1 F_2(\vec{k}_{scat},\vec{k}_{inc},\vec{\kappa}_1,\vec{\kappa}_2)\times [S_{wake}(\vec{\kappa}_1)+S_{wave}(\vec{\kappa}_1)][S_{wake}(\vec{\kappa}_2)+S_{wave}(\vec{\kappa}_2)]$$

Expanding the bracketed terms

$$\begin{aligned}\tilde{D}(\vec{k}_{scat},\vec{k}_{inc};\omega) = &\int d\vec{\kappa}_1 F_1(\vec{k}_{scat},\vec{k}_{inc},\vec{\kappa}_1)[S_{wave}(\vec{\kappa}_1)] \\ &+ \int d\vec{\kappa}_1 F_1(\vec{k}_{scat},\vec{k}_{inc},\vec{\kappa}_1)[S_{wake}(\vec{\kappa}_1)] \\ &+ \iint d\vec{\kappa}_1 d\vec{\kappa}_2 F_2(\vec{k}_{scat},\vec{k}_{inc},\vec{\kappa}_1,\vec{\kappa}_2)[S_{wake}(\vec{\kappa}_1)S_{wake}(\vec{\kappa}_2)] \\ &+ \iint d\vec{\kappa}_1 d\vec{\kappa}_2 F_2(\vec{k}_{scat},\vec{k}_{inc},\vec{\kappa}_1,\vec{\kappa}_2)[S_{wake}(\vec{\kappa}_1)S_{wave}(\vec{\kappa}_2)] \\ &+ \iint d\vec{\kappa}_1 d\vec{\kappa}_2 F_2(\vec{k}_{scat},\vec{k}_{inc},\vec{\kappa}_1,\vec{\kappa}_2)[S_{wave}(\vec{\kappa}_1)S_{wake}(\vec{\kappa}_2)] \\ &+ \iint d\vec{\kappa}_1 d\vec{\kappa}_2 F_2(\vec{k}_{scat},\vec{k}_{inc},\vec{\kappa}_1,\vec{\kappa}_2)[S_{wave}(\vec{\kappa}_1)S_{wave}(\vec{\kappa}_2)]\end{aligned}$$

Figure 5 shows (a) a typical wave spectrum, (b) a representative wake spectrum, and (c) the composite spectrum with both waves and wake present.

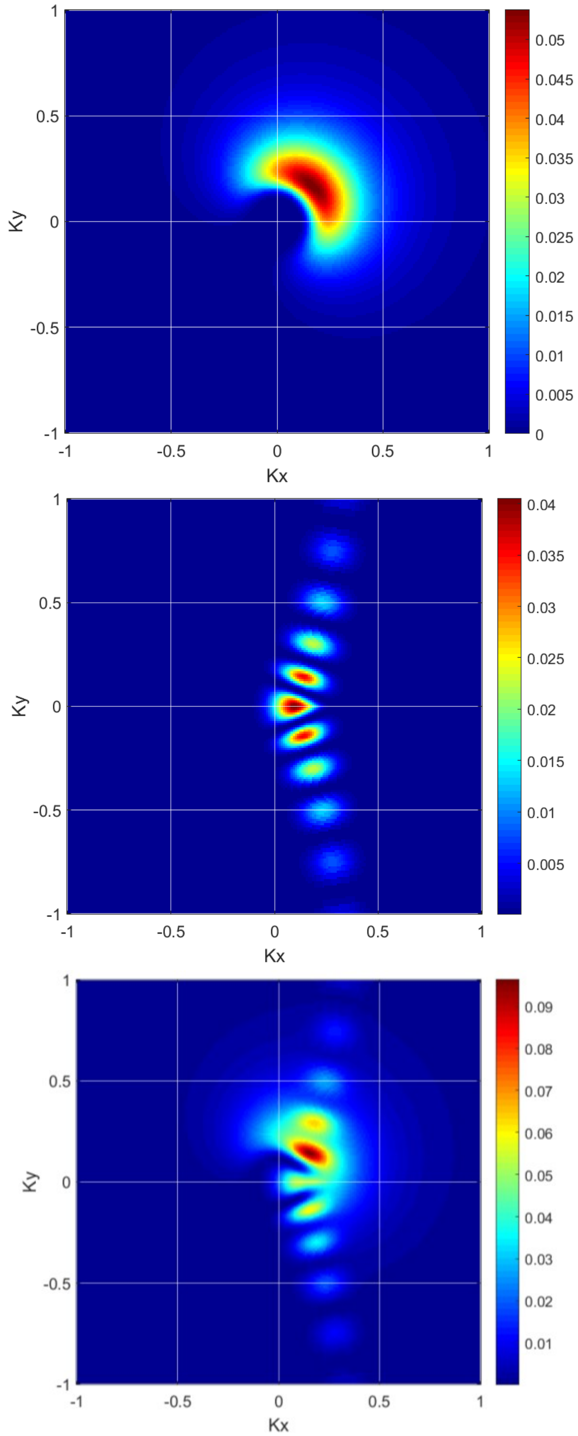

Figure 5. Directional spectra of (a) an ambient sea state, (b) a ship wake, and (c) the combined sea state

Results

Now we present results that answer the key questions posed earlier in this paper.

(i) Do wakes yield a detectable signature ?

Figure 6 shows examples of wake Doppler spectra for two frigates of rather similar dimensions, superimposed on the Doppler spectrum of the ambient sea wave spectrum. It is apparent that, in some Doppler bands, the wake Doppler power spectral density substantially exceeds that off the ambient sea and hence supports detection. The signatures are sufficiently different to support classification.

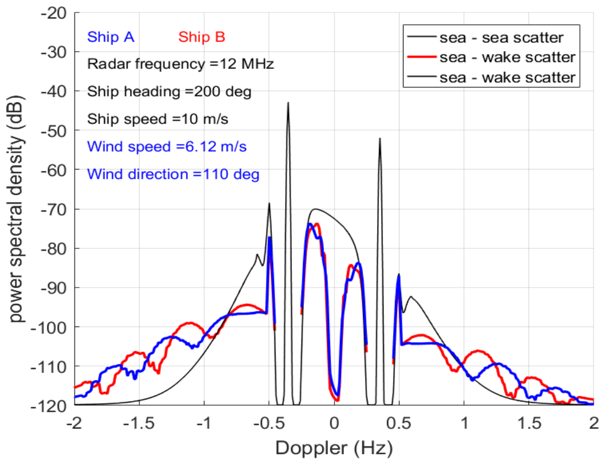

Figure 6. Comparison of the signatures of two frigates, superimposed on the ambient sea spectrum under moderate sea conditions

(ii) Are the signatures of nonlinear wave-wake interactions strong enough to yield quantitative information about the dependence of nonlinearity on wave spectral parameters ?

In Figure 7, the wake contributions to the Doppler spectrum have been separated into parts arising from (i) electromagnetic multiple scattering, and (ii) nonlinear hydrodynamic effects. The key feature here is the red curve, which plots the signature of the nonlinear hydrodynamics, while the green curve shows the sum of electromagnetic and hydrodynamic mechanisms.

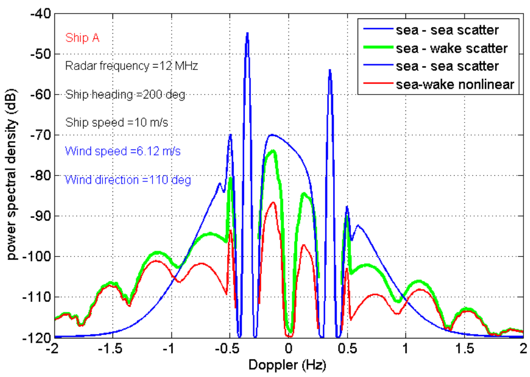

Figure 7. HF radar Doppler spectra for (i) a natural sea surface (blue), the total additional spectral energy arising from the presence of a wake (green), and (iii) the component of the wake signature due to nonlinear hydrodynamic interactions.

Conclusions

We have developed a computational model which enables us to generate the HF radar Doppler signatures associated with the Kelvin wake. The results of our initial exploration confirm both the detectability of Kelvin wakes and the potential for discrimination between ships, even when they are of similar dimensions. The parameter space is of moderately high dimensionality, and some signature features vary in a complicated, non-monotonic way with those parameters, so it will take some time and a lot of experimentation to map the corresponding structure of the signature space. But summing up the results so far, we are much encouraged.

We have also isolated the contributions arising from nonlinear wave-wake interactions. The great advantage of this kind of measurement is that the strength of the interactions can be established as a function of the wavenumber of the participating ocean wave, through exploitation of the Doppler domain.

References

[1] Anderson, S.J., HF radar signatures of ship wakes, Paper presented at the Progress in Electromagnetics Research Symposium, PIERS 2017, Singapore, October 2017.

[2] I. Carusotto & Rousseaux,G.,The Čerenkov effect revisited: From swimming ducks to zero modes in gravitational analogues," *Analogue Gravity Phenomenology* (Springer International Publishing, Heidelberg, Germany, 2013), pp. 109–144.

[3] E.O. Tuck, J.L. Collins and W.H. Wells, "On ship waves and their spectra", Journal of Ship Research, March 1971, pp.11-21

[4] E.O. Tuck, D.C. Scullen and L. Lazauskas, "Wave patterns and minimum wave resistance for high-speed vessels", 24th Symposium on Naval Hydrodynamics, Fukuoka, Japan, 8 – 13 July 2002

[5] Barrick, D.E., Remote sensing of **sea state** by radar, In Remote Sensing of the Troposphere. V.E. **Derr** (Ed.), U. S. Govt. Printing Office, 1972

[6] Anderson, S.J., & Anderson, W.C., Bistatic HF Scattering from the Ocean Surface and its Application to Remote Sensing of Seastate, Proceedings of the 1987 IEEE APS International Symposium, Blacksburg, VA, USA, June 1987.